Assessment of left ventricular diastolic suction in dogs using wave-intensity analysis

Zhibin Wang, Fereshteh Jalali, Yi-Hui Sun, Jiun-Jr Wang, Kim H. Parker and John V. Tyberg

Assessment of left ventricular diastolic suction in dogs using wave-intensity analysis

Zhibin Wang,[1] Fereshteh Jalali,[2] Yi-Hui Sun,[2] Jiun-Jr Wang,[2] Kim H. Parker,[3] and John V. Tyberg[2]

[1]*Qingdao University Medical College Hospital, Qingdao, China;* [2]*Cardiovascular Research Group, Department of Cardiac Sciences and Department of Physiology and Biophysics, University of Calgary, Calgary, Alberta, Canada; and* [3]*Department of Bioengineering, Imperial College of Science, Technology and Medicine, London, United Kingdom*

Wang, Zhibin, Fereshteh Jalali, Yi-Hui Sun, Jiun-Jr Wang, Kim H. Parker, and John V. Tyberg. Assessment of left ventricular diastolic suction in dogs using wave-intensity analysis. *Am J Physiol Heart Circ Physiol* 288: H1641–H1651, 2005. First published November 24, 2004; doi:10.1152/ajpheart.00181.2004.—Two apparently different types of mechanisms have emerged to explain diastolic suction (DS), that property of the left ventricle (LV) that tends to cause it to refill itself during early diastole independent of any force from the left atrium (LA). By means of the first mechanism, DS depends on decreased elastance [e.g., the relaxation time constant (τ)] and, by the second, end-systolic volume (V_{LVES}). We used wave-intensity analysis (WIA) to measure the total energy transported by the backward expansion wave (I_{W-}) during LV relaxation in an attempt to reconcile these mechanisms. In six anesthetized, open-chest dogs, we measured aortic, LV (P_{LV}), LA (P_{LA}), and pericardial pressures and LV volume by orthogonal ultrasonic crystals. Mitral velocity was measured by Doppler echocardiography, and aortic velocity was measured by an ultrasonic flow probe. Heart rate was controlled by pacing, V_{LVES} by volume loading, and τ by isoproterenol or esmolol administration. I_{W-} was found to be inversely related to τ and V_{LVES}. Our measure of DS, the energy remaining after mitral valve opening, I_{W-DS}, was also found to be inversely related to τ and V_{LVES} and was ~10% of the total "aspirating" energy generated by LV relaxation (i.e., I_{W-}). The size of the Doppler (early filling) E wave depended on I_{W-DS} in addition to I_{W+}, the energy associated with LA decompression. We conclude that the energy of the backward-going wave generated by the LV during relaxation depends on both the rate at which elastance decreases (i.e., τ) and V_{LVES}. WIA provides a new approach for assessing DS and reconciles those two previously proposed mechanisms. The E wave depends on DS in addition to LA decompression.

diastole; hemodynamics; mitral valve; ventricles

DIASTOLIC SUCTION (DS) is defined as that property of the left ventricle (LV) that tends to cause it to refill itself during early diastole independent of any force from the left atrium (LA). Two apparently different types of mechanistic explanations have emerged. The first type is represented by Katz (30) and Wiggers (52), who related DS to the decrease in ventricular elastance, and by several contemporary investigators (11, 12, 38, 47) who emphasized the importance of the rate of LV relaxation in subsequent diastolic filling. In 1957, Wiggers wrote that "During early moments of ventricular relaxation, elastic stresses created during contraction are released. . . If blood could enter the ventricular chamber during this phase of diastole, such a rapid drop in pressure would unquestionably constitute a potent aspirating force" (52).

Wiggers implied that the relaxing LV generates an "aspirating force" from the moment LV pressure begins to decrease. Accordingly, as elaborated upon below, the first effect of a relaxation-generated aspirating force must be to decelerate the mass represented by the stroke volume. Relaxation continues through isovolumic relaxation and only the energy remaining when the mitral valve opens can augment diastolic filling. The second proposed mechanism of DS is represented by Bloom (4, 5) and Brecher (7–9) and a number of later investigators including ourselves (1, 2, 16, 17, 22–24), who related DS to negative LV pressure (P_{LV}) and the sigmoidal nature of the diastolic LV transmural pressure-volume (P-V) relation. As LV transmural pressure (P_{LVTM}) is negative at small volumes, this explanation implies that the LV will tend to refill itself until transmural pressure (P_{TM}) is zero and that the smaller the LV end-systolic volume (V_{LVES}), the greater the DS.

Because of its ability to identify and measure upstream and downstream events and their interaction, we used wave-intensity analysis (WIA) (27, 39, 40), as we have done with respect to other hemodynamic problems (20, 21, 45). WIA provides information regarding the direction, intensity, and type of waves present at any given moment and location in a blood vessel. Because it is a time-domain analysis, wave intensity can be related temporally to hemodynamic parameters and beat-to-beat analyses can be performed (28, 39). WIA is based on the concept that "waves" [i.e., propagated disturbances (35)] that travel through the vasculature are manifested by changes in pressure and velocity (40). The energy that is transported by a wave can be quantified by measuring the changes in pressure and velocity across the wavefront (35). Waves can be either forward (i.e., in the direction of net blood flow) or backward going in direction and either compression or expansion in type. Thus there are four possible combinations: forward compression, backward compression, forward expansion, and backward expansion waves. Compression waves have a "pushing" effect and increase pressure. Forward-going compression waves increase pressure and increase velocity, whereas backward-going compression waves increase pressure and decrease velocity (in the forward direction). Expansion waves have a "pulling" effect and decrease pressure (43). Forward-going expansion waves decrease pressure and decrease velocity, whereas backward-going expansion waves decrease pressure and increase velocity (in the forward direction).

Address for reprint requests and other correspondence: J. V. Tyberg, Dept. of Cardiac Sciences and Dept. of Physiology and Biophysics, Univ. of Calgary, Health Sciences Centre, 3330 Hospital Dr. NW, Calgary, Alberta, Canada T2N 4N1 (E-mail: jtyberg@ucalgary.ca).

Thus, according to WIA, blood in the cardiovascular system is accelerated or decelerated by forward- or backward-going compression or expansion waves (28). At the beginning of systolic ejection, the LV generates a compression wave that accelerates stroke volume and, after the LV begins to relax, an expansion wave that decelerates stroke volume, reducing aortic flow to zero and causing the aortic valve to close. During isovolumic relaxation, the falling ventricular pressure generates self-cancelling forward and backward expansion waves. When the mitral valve opens, the backward expansion wave, which continues until P_{LV} reaches a minimum, propagates into the atrium and initiates diastolic filling. Only the fraction of the total energy of this expansion wave that remains at the opening of the mitral valve can augment diastolic filling.

Therefore, the purpose of this study was to measure the total "aspirating energy" (i.e., I_{W-}; see below) associated with LV relaxation and to test the hypothesis that I_{W-} depends on both the rate at which elastance decreases [as measured by the exponential time constant of LV relaxation (τ)] and the completeness of LV emptying (as measured by V_{LVES}). In addition, we measured the fraction of I_{W-} expended in decelerating the stroke volume at the end of systolic ejection, the fraction associated with isovolumic relaxation, and the fraction available to accelerate mitral inflow. Finally, we studied the acceleration phase of the Doppler E wave and related its magnitude to its possible causes [i.e., the "push" from the decompressing left atrium (LA) and/or the "pull" from the relaxing LV, a.k.a. DS].

Glossary

BCW	Backward compression wave
BEW	Backward expansive wave
c	Wave speed (m/s)
dI_W	Net intensity [W/m^2; ($dI_{W+} - dI_{W-}$), formerly called dPdU]
dI_{W+}	Intensity (W/m^2) of a forward-going wave
dI_{W-}	Intensity (W/m^2) of a backward-going wave
dP	Incremental change in pressure during the sampling interval at any time and location
dU	Incremental change in velocity during the sampling interval at any time and location
D_{AP}	Anterior-posterior dimension
D_{LA}	Long-axis dimension
D_{SL}	Septal-lateral dimension
DS	Diastolic suction
ED	End diastole (diastolic)
ES	End systole (systolic)
EVI_{ACC}	Time integral of the acceleration phase of the early velocity waveform
FCW	Forward compression wave
FEW	Forward expansive wave
HR	Heart rate (beats/min)
I_{W-}	Energy (J/m^2) of a backward-going wave
LA	Left atrium (atrial)
LV	Left ventricle (ventricular)
P	Pressure [pascals (N/m^2) in equations and mmHg in plots]
P_{Ao}	Aortic pressure
P_{LA}	LA pressure
P_{LV}	LV pressure
P_{LVED}	LV end-diastolic pressure
P_{LVTM}	LV transmural pressure
P_{Peric}	Pericardial pressure
P_{TM}	Transmural pressure (i.e., inside minus outside pressure)
U	Velocity (m/s)
V	Volume
V_0	Equilibrium volume, the volume contained by a structure when $P_{TM} = 0$
V_{LV}	LV volume
V_{LVES}	LV end-systolic volume
WIA	Wave-intensity analysis
ρ	Density (kg/m^3)
τ	Exponential time constant of the decrease in P_{LV} (i.e., relaxation)

MATERIALS AND METHODS

Animal preparation. With the use of a protocol approved by the institutional animal care committee, the experiments were performed on six healthy mongrel dogs weighing between 21 and 25 kg using standard open-chest surgical techniques previously described (14, 18). Dogs were anesthetized by thiopental sodium followed by fentanyl citrate and ventilated with a constant-volume respirator to maintain normal blood gas tensions and pH. P_{Ao}, P_{LV}, P_{LA}, and P_{Peric} (19, 42) were measured using catheter-tip manometers (Millar; Houston, TX). The catheter-tip manometers were referenced using their fluid-filled lumens so that absolute values of pressure could be ascertained. Three pairs of ultrasonic crystals were implanted in the LV endocardium to measure D_{AP}, D_{SL}, and D_{LA} (in one dog, it was not possible to measure D_{LA} so the product of D_{AP} and D_{SL} was used as an index of V_{LV}). The velocity of blood flowing through the mitral orifice was measured using a Doppler echocardiographic system (model 77020AC, Hewlett-Packard; Palo Alto, CA). A 5-MHz transesophageal transducer was placed on the surface of the heart, and an apical two- or four-chamber view was recorded. Mitral inflow velocity was then measured using pulsed-wave Doppler echocardiography with the sample volume cursor positioned at the level of the mitral tips. Visualization was optimized (i.e., we attempted to achieve the highest velocity with least spectral dispersion) by adjusting the controls of the transducer. Doppler echocardiographic and catheter hemodynamic data were synchronized using a frame counter developed in our laboratory. Aortic flow was measured using an ultrasonic flowmeter (Transonic Systems; Ithaca, NY); velocity was calculated using the nominal diameter of the probe. A signal from the ventilator was recorded to indicate end-expiration. After the administration of UL-FS-49 (26) (Boehringer Ingelheim Pharmaceuticals; Ridgefield, CT), HR was controlled by right atrial pacing. The dog's temperature was monitored and maintained with the aid of a heating pad and lamp. The surgical preparation required ~90 min and, after a 30-min equilibration period, collection of the data required ~2 h.

Experimental protocol. The rationale of our protocol was to acquire a "three-dimensional" matrix of data by systematically manipulating three independent variables [P_{LVED} (as a means of changing V_{LVES}), HR, and τ] through wide ranges. Starting at $P_{LVED} = 10$ mmHg, HR was increased continuously from 90 to 130 beats/min. We then gave esmolol (0.1 mg/kg LV bolus) and repeated the HR manipulation. Next, after allowing several minutes for recovery, we gave isoproterenol (0.3 μg/kg LV bolus) and repeated the HR manipulation again. P_{LVED}s of 15, 20, and 25 mmHg were achieved by infusing volume (an albumin-Ringer lactate solution). At each volume level, we recorded a series of transmural P-V loops during blood withdrawal and/or constriction of the posterior vena cava. At each level of P_{LVED}, the same HR and esmolol-isoproterenol interventions were performed. This provided a range of τ at the control and extreme values of both

V_{LVES} and HR, thus describing a matrix of data in terms of the independent variables (i.e., HR, τ, and P_{LVED}). Between each intervention, enough time was allowed for hemodynamic stability to be reestablished. Data were recorded using a computer system (Sonometrics; Ontario, Canada); each data-acquisition period lasted $\sim$2 min.

Data processing and analysis. The digitized data were analyzed (CVSOFT, Odessa Computer System; Calgary, Alberta, Canada); hemodynamic values were obtained by averaging the data obtained during steady-state recording intervals that spanned at least three expiratory cycles.

ED was defined as the relative minimum in P_{LV} that followed the A wave. End-ejection (i.e., ES) was defined by the incisura in the P_{Ao} waveform. P_{LVTM} equalled ($P_{LV} - P_{Peric}$). V_{LV} was modelled as a modified general ellipsoid using the following formula: $V_{LV} = (\pi/6) \cdot D_{AP} \cdot D_{SL} \cdot D_{LA}$. V_{LVES} was normalized by the LV V_0 for each dog [i.e., V_{LVES} (%) = (V_{LVES} / V_0) $\cdot$ 100]. V_0 (the zero-pressure intercept of the end-diastolic P-V relationship) was estimated by first collecting a series of P_{LVTM} and V_{LV} data points and then characterizing the plot with two logarithmic curves (one for each of the positive and negative portions of the P_{LVTM}-V_{LV} relation) (37). τ was determined by fitting the data from minimum dP_{LV}/dt to mitral valve opening to the following equation: $P(t) = P_A \cdot e^{-t/\tau} + P_B$, where t is the time from minimum dP_{LV}/dt, P_A is P_{LV} at that instant, and P_B is P_{LV} when $t = \infty$.

To determine the degree to which relaxation was complete at the time of mitral valve opening, we expressed that value of P_{LV} as a fraction of the difference between the asymptotic value (P_B) and the end-systolic value.

The intensity of the wave that travelled backward from the LV was calculated using the following formula: $dI_{W-} = -(4\rho c)^{-1}(dP - \rho c dU)^2$, where ρ is the density of blood (kg/m^3), c is the wave speed (m/s), dP is the incremental difference in P_{LV} (1 mmHg = 133 N/m^2) during a 5-ms sampling interval, and dU is the difference in mitral velocity (m/s) (40). The intensity of the wave that travelled forward from the LA was calculated using the following formula: $dI_{W+} = (4\rho c)^{-1}(dP + \rho c dU)^2$. Wave speed was calculated continuously throughout the cardiac cycle using the following equation: $c = (ElA/\rho)^{0.5}$ (50). [We compared these values to that estimated as $c = dP/\rho dU$ (39), particularly examining the value at the beginning of LV filling when reflections can be expected to be minimal, and found excellent agreement.] Elastance (E) was defined as $E = P_{LV}/(V_{LV} - V_d)$, where V_d is the zero-pressure intercept of the end-systolic P-V relationship, l is length and equalled D_{LA}, and A is area and equalled $(\pi/4)(D_{AP} \cdot D_{SL})^2$. Because the end-systolic P-V relationship had not been explicitly defined by caval constriction in most dogs, V_d was assumed to be 72% of V_0 based on data from a subset of three dogs.

For this study, we adopted the convention that LV inflow velocities (i.e., the mitral E and A waves) should be given positive values and LV outflow velocity (i.e., aortic flow divided by estimated cross-sectional area) should be given a negative value (see Fig. 1).[1] Thus the dI_{W-} waveform (W/m^2, power per unit cross-sectional area of the backward-going expansion wave) described the instantaneous aspirating power associated with LV relaxation (52). We calculated the total time integral under (i.e., between the waveform and zero) the dI_{W-} waveform [I_{W-} (J/m^2), energy per unit cross-sectional area] to calculate the total aspirating energy. To determine the fraction of the total aspirating energy that was expended as hydraulic work to decelerate the aortic column of blood, we plotted the area under the dI_{W-} waveform until ES (dotted area) versus the total I_{W-} and determined the average fraction by linear regression (forced through the origin).

Fig. 1. WIA of a cardiac cycle. Isovolumic intervals are indicated by thin vertical lines. *Top*: P_{Ao}, P_{LV}, and P_{LA} and aortic (U_{Ao}; calculated from flow) and mitral (U_{Mi}; Doppler) velocities. *Top middle*: intensity of forward- (dI_{W+}) and backward-going (dI_{W-}) waves and net intensity (dI_W; thick solid line). During relaxation, the LV generated a backward-going expansion wave (BEW) that began at the moment P_{LV} and E began to decline, then increased rapidly, and reached a peak when dP_{LV}/dt (not shown) reached its largest negative value. The component related to early diastolic mitral flow acceleration was relatively small. *Bottom middle*: dI_{W+} and dI_{W-} at greater sensitivity. BCW, backward-going compression wave. *Bottom*: time course of I_{W-}, the time integral of dI_{W-}, during LV relaxation.

Likewise, to determine the fraction of the total aspirating energy that was expended as hydraulic work to accelerate the mitral column, we plotted the area under the dI_{W-} waveform described after the beginning of mitral flow (diagonally hatched area) versus I_{W-} and determined that average fraction. Similarly, we plotted the area under the dI_{W-} waveform during isovolumic relaxation (oppositely hatched area) (of course, this energy could not be converted to hydraulic work because there was no flow) versus I_{W-} and determined that average fraction also. Each of these energies was expressed as an average fraction of the total energy, I_{W-}. To determine the energy due to the passive decompression of the LA, we calculated the area (I_{W+}) under the dI_{W+} waveform during the E wave (see FCW in Fig. 1, *bottom middle*). In addition, the time integral of the early filling velocity

---

[1] By this convention, the waves generated by the LV propagating out of the ventricle either into the aorta or the atrium will be seen as backward waves. For the systolic part of the cardiac cycle, this is opposite to the convention that we have adopted in our previous studies of wave intensity measured in the aorta.
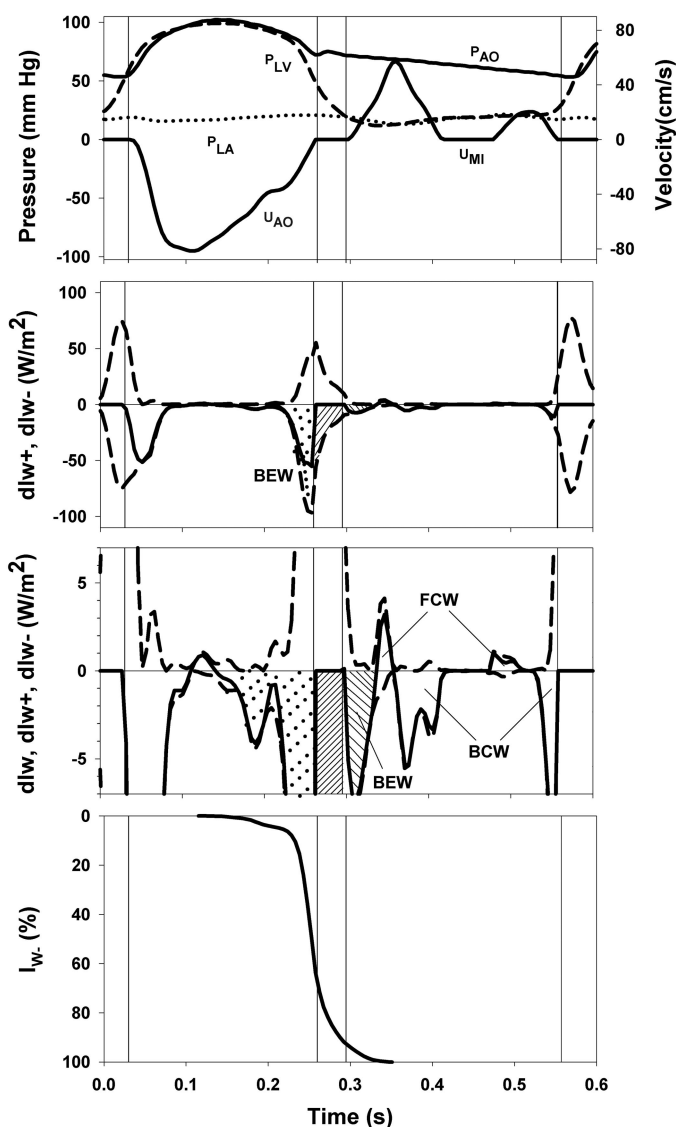
waveform (i.e., the E wave) during its acceleration phase (EVI$_{ACC}$; i.e., until the peak of the E wave) was measured.

There is, perhaps, a conceptual difficulty in the application of WIA to the LV during the isovolumic periods when no waves can propagate into or out of the ventricle because the valves are closed. We believe that this difficulty can be overcome by an extension of the analysis of wave behavior at the closed end of a tube, where the boundary condition of no flow requires that the reflection coefficient equals +1. (In such a tube, the magnitude of the incident wave equals that of the reflected one, i.e., $dP_+ = dP_-$ and $dU_+ = -dU_-$). Therefore, the energy of the incident backward-going expansion wave generated by the relaxing myocardium arriving at the closed mitral valve must be equal to the energy of the reflected forward-going expansion wave, which will have the same absolute value but the opposite sign [$dI_{W\pm} = \pm(4\rho c)^{-1}(dP)^2$]. The net intensity ($dI_W = dPdU$) is zero because the velocity must be zero at the closed valve. This zero net wave intensity is interpreted as the result of equal and opposite intensities of forward- and backward-going waves, as shown in Fig. 1, *top middle*.

Results are expressed as means ± SD. One-way ANOVA was used to compare the variables between different P$_{LVED}$ levels. Linear and nonlinear regression analyses were performed to explore the interaction between different variables. A probability level of $P < 0.05$ was accepted as significant.

RESULTS

Pooled data from six dogs at four different levels of P$_{LVED}$ (10, 15, 20, and 25 mmHg) are shown in Table 1. P$_{LA}$ was elevated ($P < 0.001$) in parallel with the increase in P$_{LVED}$. V$_{LVES}$ and V$_{LVED}$ increased significantly, as did P$_{LVED\ TM}$ (all $P < 0.001$). There was no statistically significant increase in τ ($P = 0.1$). EVI$_{ACC}$ increased significantly ($P < 0.01$). dI_{W-} significantly decreased in absolute value when P$_{LVED}$ was elevated ($P = 0.02$), as did I_{W-} ($P = 0.04$) and I_{W-DS} ($P = 0.04$).

Analysis of the effects of HR, τ, and V$_{LVES}$ on I_{W-} demonstrated that τ and V$_{LVES}$ were the only independent determinants of I_{W-}. Analysis of each dog's data (Fig. 2) and the pooled data (see Fig. 4A) showed an inverse relationship between %V$_{LVES}$ and I_{W-}: as %V$_{LVES}$ decreased, I_{W-} increased. We used a three-parameter exponential decay equa-

tion [$I_{W-} = a \cdot e^{b(\%V_{LVES})} + (I_{W-})_\infty$] and found that, in the case of each dog's data, the 95% confidence intervals of b did not include zero, indicating that the exponential term was significant (see Table 2). Similar inverse relationships were found between I_{W-} and τ: as τ decreased, I_{W-} increased (Figs. 3 and 4B). In this case as well, we used a similar equation [$I_{W-} = a \cdot e^{b\tau} + (I_{W-})_\infty$] and also found that, in every experiment, the 95% confidence intervals of b did not include zero, indicating that the exponential term was significant (see Table 2). In addition to the above statistical justification for using a nonlinear regression, we noted that, in the case of a linear regression, extrapolation would suggest that I_{W-} would go through zero and change its sign at high values of τ or V$_{LVES}$, which seemed unreasonable, a priori. Conversely, extrapolation of an exponential decay would suggest that I_{W-} would plateau and reach asymptotic levels at high values of τ and V$_{LVES}$. It was found that variance could further be reduced (i.e., both coefficients were statistically significant) when both τ and V$_{LVES}$ were used to predict I_{W-}; this indicated that the combination of τ and V$_{LVES}$ predicted I_{W-} better than either one alone (Fig. 5A). Note that τ and V$_{LVES}$ data were distributed quite uniformly (Fig. 5B).

dI_{W-} as a measure of aspirating energy. As shown by the second peak in the dI_{W-} waveform in Fig. 1, *top middle*, the LV generates a large, backward-going expansion wave during relaxation; the wave begins at the moment P$_{LV}$ and E begin to decline, then rapidly increases in absolute value, and reaches a peak approximately at the time when dP_{LV}/dt reaches its minimum value. dI_{W-} then declines through isovolumic relaxation and early diastolic filling. To determine the fractions of the total aspirating energy associated with aortic deceleration, isovolumic relaxation, and mitral filling, these respective areas were plotted versus the total area (I_{W-}; Fig. 6). Linear regression analysis indicated that the fractions were 0.59, 0.32, and 0.08, respectively.

The component related to early diastolic mitral flow acceleration (i.e., dI_{W-DS}) is only ~10% of the total time-integrated area of the waveform. However, like I_{W-} and consistent with

Table 1. *Hemodynamic data*

	P$_{LVED}$ mmHg				
	10	15	20	25	*P* Value
n	22	34	41	25	
P$_{LVED}$, mmHg	10.7±1.0	14.8±1.5	20.1±1.5	24.8±1.5	
P$_{Peric}$, mmHg	6.1±2.4	9.5±1.9	12.8±2.2	16.7±1.3	<0.001
P$_{LVED\ TM}$, mmHg	2.4±2.2	4.0±1.9	6.2±1.4	8.5±1.8	<0.001
P$_{LA}$, mmHg	10.6±2.2	13.0±3.3	17.1±3.8	18.2±4.0	<0.001
V$_{LVED}$, %V$_0$	104.1±15.6	104.9±12.7	113.0±15.7	139.0±14.3	<0.001
V$_{LVES}$, %V$_0$	82.5±11.3	84.8±9.8	86.6±11.4	103.6±11.9	<0.001
τ, ms	22.0±13.3	21±12.3	23±9.8	20±11.3	0.1
EVI$_{ACC}$, cm	1.5±0.5	1.6±0.4	1.9±0.3	1.7±0.4	0.01
dI_{W-}, W/m^2	−91.5±36.1	−78.1±26.8	−79.0±32.7	−64.6±27.3	0.02
I_{W-}, J/m^2	−4.6±2.4	−3.9±1.8	−4.4±2.5	−2.9±2.0	0.02
I_{W-DS}, mJ/m^2	−358±169	−336±206	−352±179	−298±180	0.04
I_{W+}, mJ/m^2	40±20	38±20	46±20	46±21	0.04

Values are means ± SD; *n*, no. of animals. P$_{LVED}$, left ventricular (LV) end-diastolic pressure; *P*, probability of a significant difference as determined by one-way ANOVA; P$_{Peric}$, end-diastolic pericardial pressure; P$_{LA}$, left atrial (LA) pressure at mitral valve opening; P$_{LVED\ TM}$, LV end-diastolic transmural pressure; V$_{LVED}$, LV end-diastolic volume; V$_0$, LV equilibrium volume; V$_{LVES}$, LV end-systolic volume; τ, exponential constant of LV relaxation; EVI$_{ACC}$, time integral during the acceleration phase of the E wave; dI_{W-}, peak value of the intensity of the backward-going wave; I_{W-}, time integral of the intensity of the backward-going wave; I_{W-DS}, component of the time integral of the intensity of the backward-going wave that is related to acceleration of early diastolic mitral flow; I_{W+}, time integral of the intensity of the forward-going compression wave that is related passive LA decompression.
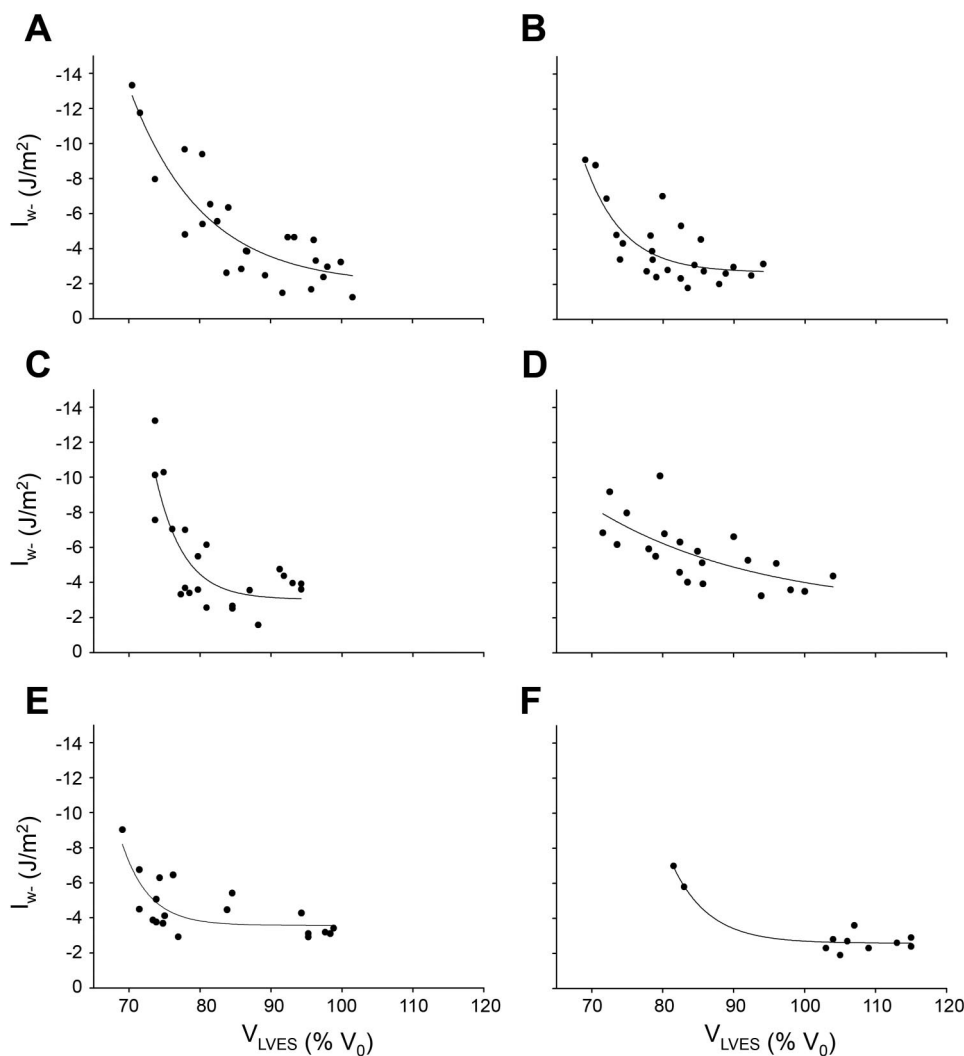
Fig. 2. I_{W-} plotted against normalized V_{LVES} (%V_0) for each dog (*A–F*). Data were fitted to a three-term exponential equation: $I_{W-} = [a \cdot e^{b(\%VLVES)}] + (I_{W-})_\infty$. Parameter values are shown in Table 2.

the constant proportionality demonstrated in Fig. 6, I_{W-DS} varied inversely with τ and V_{LVES} (Fig. 7).

We found that, at the time of P_{LV}-P_{LA} crossover (i.e., mitral valve opening), P_{LV} had declined to $86 \pm 6\%$ of the difference between P_{LVES} and the asymptotic value (P_B).

Determinants of E wave acceleration. As illustrated in Fig. 1, *bottom middle*, a FCW began just after P_{LV} reached its nadir, when mitral velocity was continuing to increase. The energy (I_{W+}) of this FCW, which would tend to force blood into the LV, was attributed to the passive emptying of a stretched LA.

Blood is also drawn into the LV by the remaining aspirating energy (I_{W-DS}). Thus, to determine the relative contributions of this LA push and LV pull, we applied multiple linear regression, considering EVI_{ACC} to be the dependent variable and I_{W+} and I_{W-DS} to be independent variables (Fig. 8). Both I_{W+} and I_{W-DS} predicted EVI_{ACC} in that they both reduced variance statistically significantly. These results suggest that early diastolic filling (as measured by EVI_{ACC}) was determined by both the passive push of the LA (as measured by I_{W+}) and the active pull of the LV (as measured by I_{W-DS}). A 1-cm

Table 2. *Nonlinear regression parameters*

| Dog | $I_{W-} = a \cdot e^{b(\%VLVES)} + (I_{W-})_\infty$ | | | | $I_{W-} = a \cdot e^{b\tau} + (I_{W-})_\infty$ | | | |
	a, J/m²	b, %$^{-1}$	$(I_{W-})_\infty$, J/m²	r^2	a, J/m²	b, ms^{-1}	$(I_{W-})_\infty$, J/m²	r^2
A	-100 ± 204	-0.10 ± 0.03	-1.9 ± 1.1	0.77	-20 ± 4	-0.07 ± 0.02	-2.2 ± 1.0	0.77
B	-204 ± 760	-0.18 ± 0.07	-2.7 ± 0.6	0.65	-136 ± 103	-0.23 ± 0.06	-3.2 ± 0.6	0.83
C	-850 ± 190	-0.25 ± 0.00	-3.0 ± 0.5	0.70	-13 ± 4	-0.07 ± 0.03	-2.9 ± 1.1	0.61
D	-518 ± 160	-0.13 ± 0.05	-4.1 ± 0.6	0.73	-101 ± 154	-0.14 ± 0.08	-2.2 ± 0.8	0.58
E	-411 ± 961	-0.27 ± 0.00	-3.6 ± 0.4	0.56	-11 ± 4	-0.09 ± 0.06	-3.5 ± 1.2	0.58
F	-263 ± 206	-0.16 ± 0.11	-2.5 ± 0.3	0.92	-3.24 ± 425	-0.32 ± 0.10	-2.5 ± 0.2	0.88
Pooled data	-135	-0.11	-2.9	0.45	-16	-0.08	-3.0	0.57

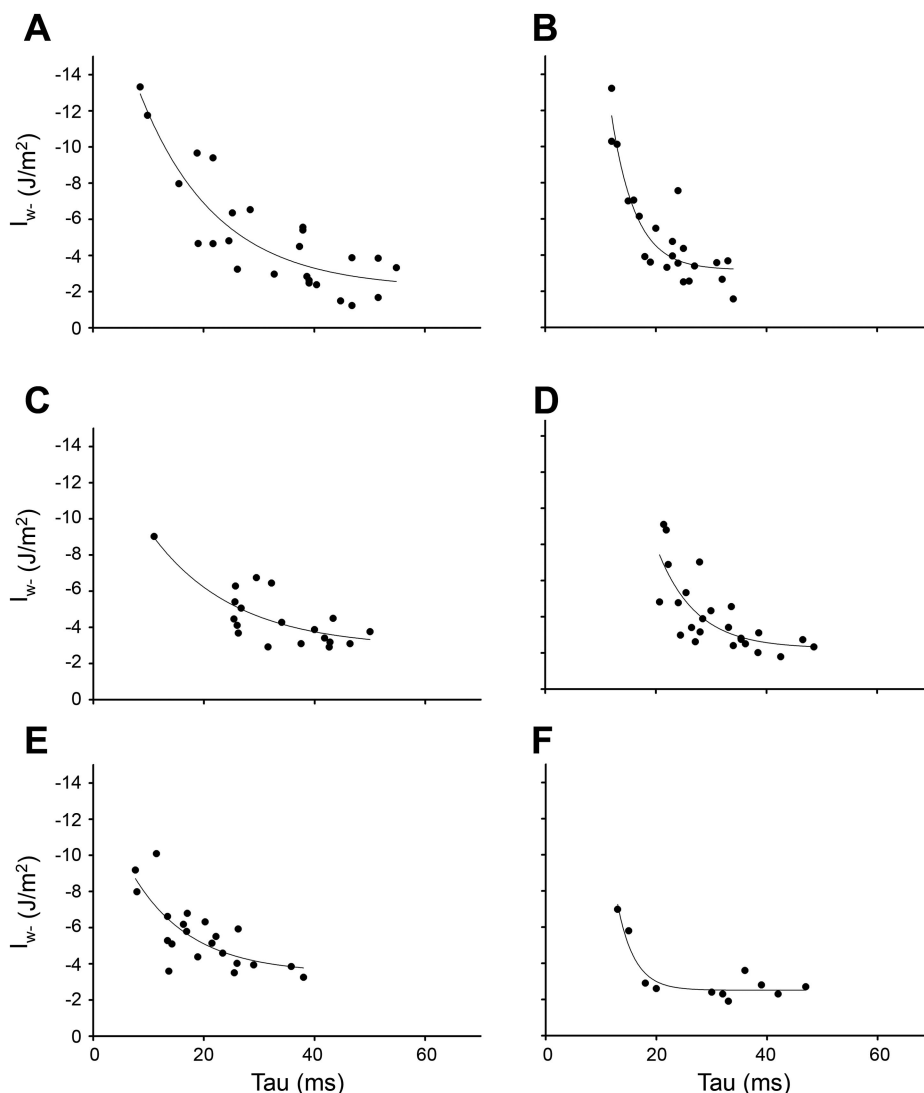Values are regression values $\pm$ 95% confidence intervals.

Fig. 3. I_{W-} plotted against τ for each dog (*A–F*). Data were fitted to a three-term exponential equation: $I_{W-} = a \cdot e^{b\tau} + (I_{W-})_\infty$. Parameter values are shown in Table 2.

increase in EVI_{ACC} was associated with a 0.08 J/m^2 increase in I_{W+} and a 1.7 J/m^2 increase in I_{W-DS}. Thus the LV expends ~20 times more energy to accelerate the mitral flow than the LA.

DISCUSSION

The major conclusion of this investigation is that the relaxing LV generates an expansion wave that first decelerates the stroke volume moving through the aorta, then rapidly declines in magnitude during isovolumic relaxation, and finally accelerates blood in the mitral inflow tract. The total energy of that expansion wave (I_{W-}) and the energy remaining after the mitral valve opens (I_{W-DS}) were demonstrated to be inversely related to the rate at which P_{LV} decreases (i.e., τ). This demonstration fulfills Wiggers' anticipation that decreasing P_{LV}, per se, is capable of generating an aspirating force (52) and is consistent with the interpretation of those investigators who have emphasized the significance of the rate of relaxation as a determinant of DS (11, 12, 30, 38, 47). The total energy of that expansion wave (I_{W-}) and the energy remaining after the mitral valve opens (I_{W-DS}) were also demonstrated to be inversely

related to the completeness of LV emptying (i.e., V_{LVES}). This demonstration is consistent with that body of work that relates DS to LV V_0 (1, 2, 4, 5, 7–10, 16, 17, 22–24, 37, 44, 48). Thus analysis of the energy of the backward-going, LV-generated, expansion wave seems to reconcile the two apparently unrelated mechanisms of DS that had been proposed previously.

As the backward-going expansion wave generated by the relaxing LV began at the moment P_{LV} and *E* began to decline, its onset coincided with the beginning of Wiggers' "phase of reduced ejection" (51), an instant substantially later than the peak of the calcium transient (25). dI_{W-} then increased rapidly (in absolute value) and reached a peak near the time when dP_{LV}/dt reached its largest negative value. dI_W (net intensity, a.k.a. $dPdU$) is equal to the sum of dI_{W+} and dI_{W-}, and its sign (positive or negative) indicates whether the forward or backward wave is dominant at that instant. In Fig. 1, *bottom middle*, note that dI_W began to increase when the mitral valve opened and declined to zero when dP_{LV}/dt equalled zero (36). This implies that the backward-going expansion wave was no longer dominant after P_{LV} reached its minimum value, thus corresponding precisely to Katz's conclusion that the LV tends to
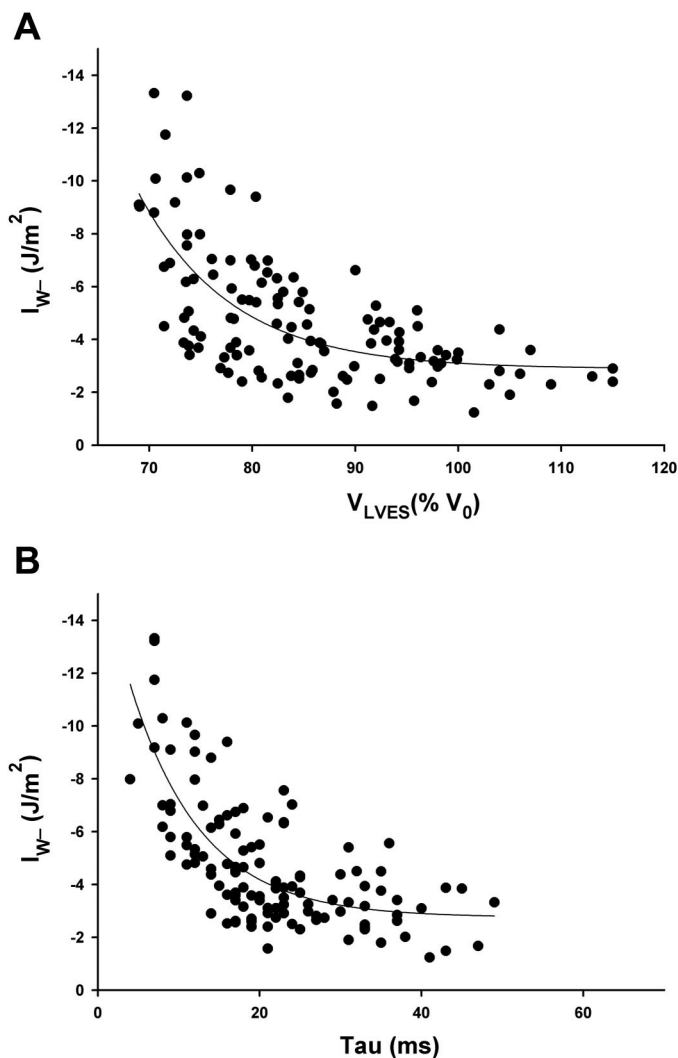
A

B

Fig. 4. *A*: I_{W-} plotted against normalized V_{LVES} (%V_0); pooled data are from 6 dogs. *B*: I_{W-} plotted against τ; pooled data are from 6 dogs. Parameter values are shown in Table 2.

the use of WIA to separate the measured pressure and velocity waveforms into their forward and backward components with no presumptions about the origins of these waves. A number of models of LV filling have been suggested, ranging from one-dimensional parametric models (6, 15, 46) through two-dimensional models (49) to fully three-dimensional models (32). All of these models require prior knowledge about the properties and state of the ventricle to enable the prediction, to different levels of complexity, of the mitral filling pattern. Our work, on the other hand, is primarily descriptive rather than
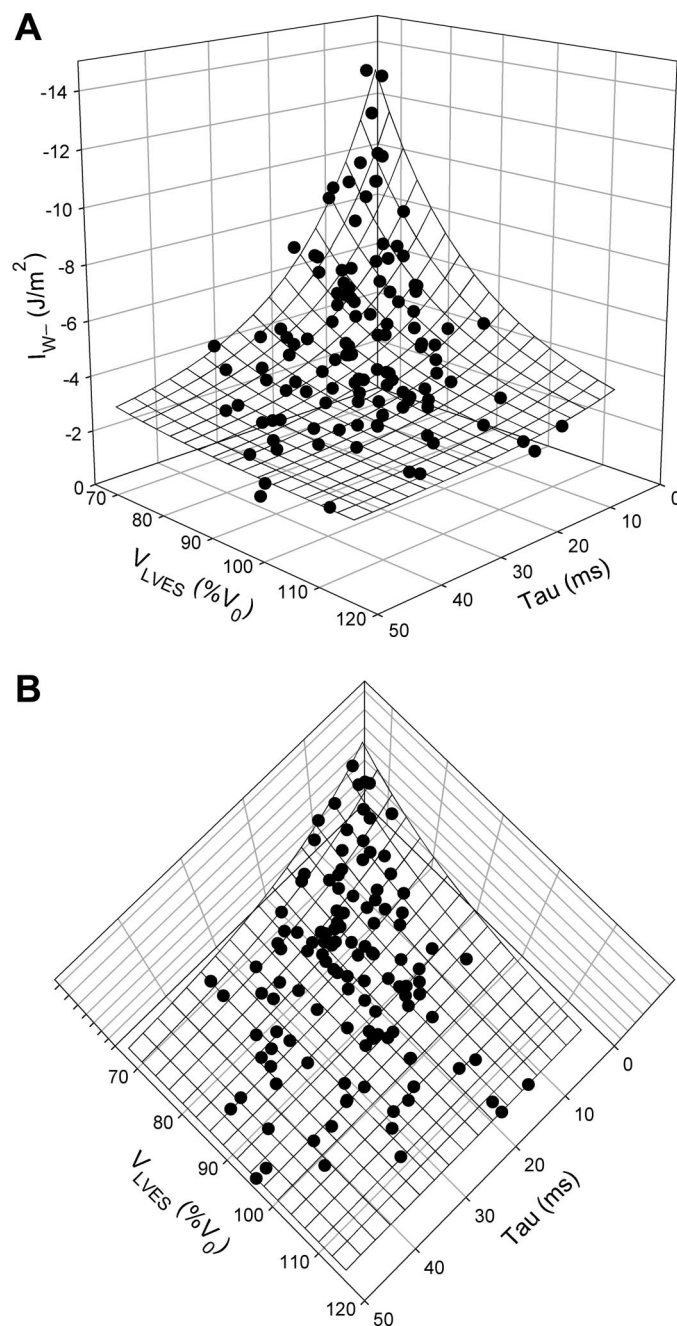
A

B

Fig. 5. *A*: 3-dimensional mesh plot showing the nonlinear relations between I_{W-} and τ and V_{LVES}. $I_{W-} = -505(e^{-0.05\,\tau})[e^{-0.06(\%VLVES)}] - 3$. $r^2 = 0.69$. *B*: plot of τ versus V_{LVES} demonstrating the uniformity of the data distribution. Pooled data are from 6 dogs.

fill itself until the nadir in P_{LV} (12, 30, 38, 47). Katz analyzed the early phase of diastolic filling and concluded that the fact that P_{LV} decreased during early filling meant that the LV was filling itself. Because LV *E* (i.e., the slope of a line drawn from the origin to a point on the P-V loop) decreased continuously during this period, he inferred that the LV was relaxing faster than it could be filled and, so, was responsible for its own filling (30).

Figures 2 and 4*A* demonstrate the dependence of dI_{W-} on V_{LVES}, and it is important to note that, despite the vigorous volume loading in this experimental protocol, most values of V_{LVES} were less than V_0 (see Table 1). This implies that these hearts usually emptied to volumes that were less than their V_0 and suggests that the V_0 mechanism may be an important factor in LV filling under a wide range of loading conditions. However, it should be noted that our protocol did not include the study of ventricles made markedly hypovolemic except by increasing contractility.

It should be emphasized that we are not attempting to model the mechanics of the LV in this study. We are simply exploring
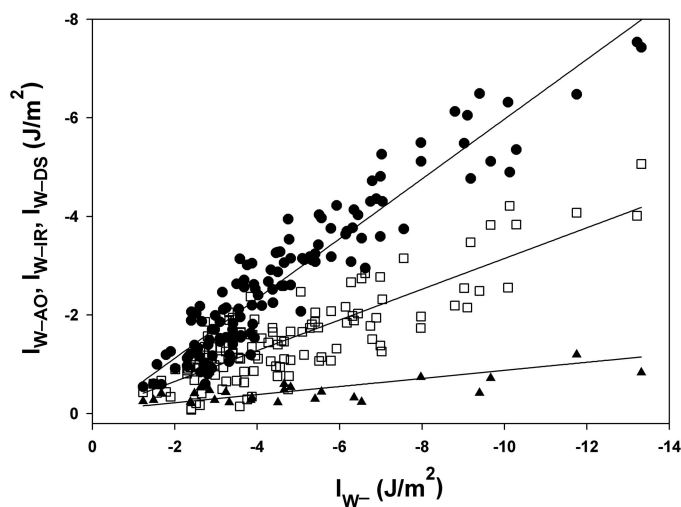
Fig. 6. Fractions of the total aspirating energy (I_{W-}) associated with aortic deceleration (I_{W-Ao}; ●), isovolumic relaxation (I_{W-IR}; □), and mitral filling (I_{W-DS}; ▲) plotted versus I_{W-} (see Fig. 1). Results of linear regression (forced through the origin) are as follows: $I_{W-Ao} = 0.59I_{W-}$, $I_{W-IR} = 0.32I_{W-}$, and $I_{W-DS} = 0.08I_{W-}$. Pooled data are from 6 dogs.

Fig. 8. Three-dimensional mesh plot showing the relations between the acceleration portion of the Doppler E wave (EVI_{ACC}), I_{W-DS}, and I_{W+} attributed to passive LA decompression (see Fig. 1). $EVI_{ACC} = 9.7 I_{W+} - 0.4I_{W-DS} + 1.1$. $r^2 = 0.44$. These results suggest that early diastolic filling (as measured by EVI_{ACC}) was determined by both the active "pull" of the LV (as measured by I_{W-DS}) and the passive "push" of the LA (as measured by I_{W+}). Pooled data are from 6 dogs.

predictive. Of course, the findings do have implications for the modeling of ventricular filling and these have been discussed as appropriate. Similarly, the simultaneous measurement of pressure and velocity in the ventricle is highly invasive and does not lend itself easily to clinical measurements. However, insofar as physiological measurements taken in the open-chested dog are relevant to the human cardiovascular system, the findings of our work do have clinical implications and these will be discussed briefly.

Previously, it was suggested that DS is related to the untwisting of the LV (3, 33, 41), so it is interesting to note that the time course of I_{W-} is similar to that of LV
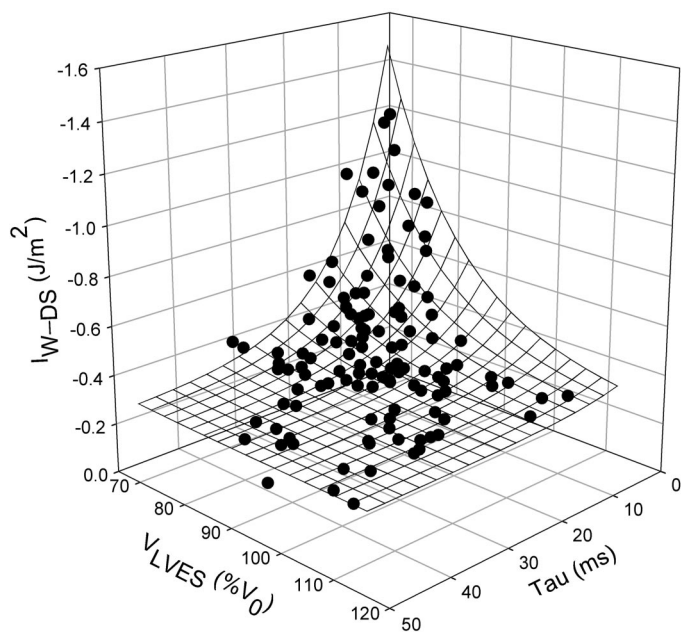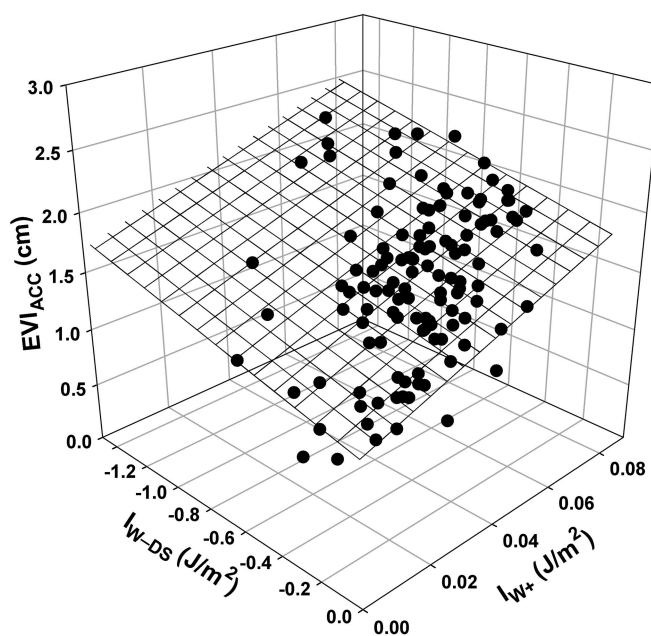

Fig. 7. Three-dimensional mesh plot shows the nonlinear relations between I_{W-DS} and τ and V_{LVES}. $I_{W-DS} = -181(e^{-0.11\ \tau})[e^{-0.067(\%VLVES)}] - 0.30$. $r^2 = 0.59$.

untwisting: both the backward expansion wave and untwisting are largely complete by the time the mitral valve opens (see Fig. 1, *bottom*). On one hand, this might suggest that neither I_{W-} nor untwisting is as directly related to early mitral filling as had been supposed. On the other hand, with Wiggers' aspirating force perspective in mind, it might also suggest that both I_{W-} and untwisting are intimately related to the decrease in LV E and to V_{LVES} (33, 41). Furthermore, it might suggest that both I_{W-} and untwisting are related in a major way to the deceleration of the stroke volume and to early mitral filling, the latter, in a perhaps still critically important way, despite the fact that I_{W-DS} is small. Thus, like the earlier authors, we conclude that the relaxation of the "torsional spring" is the likely cause of the decrease in E and the backward-going expansion wave (I_{W-}), ~10% of which we equate to DS (I_{W-DS}).

Mitral filling. We also examined the degree to which DS affects mitral filling. Wiggers acknowledged that the aspirating force would tend to augment mitral filling but emphasized that P_{LV} is nearly at its nadir when the mitral valve opens and, therefore, only a small fraction of that force would be available for diastolic filling (52). (Our data demonstrated that relaxation was ~86% complete when the mitral valve opened.) However, our data also demonstrated that there was an association between the size of the E wave and I_{W-DS} in addition to I_{W+} (see Fig. 7). Although both associations were statistically significant, I_{W-DS} was ~20 times greater in magnitude than I_{W+}, suggesting that LV DS is more important than the passive decompression of the LA in determining the size of the E wave. These findings suggest that the role of DS should be evaluated carefully when assessing LV diastolic function

in both normal subjects and those with congestive heart failure (29).

Deceleration of aortic flow. Wiggers' discussion of the aspirating force (52) would seem to suggest that its first effect is to decelerate, stop, and reverse the column of blood in the aortic outflow tract. Under a variety of loading conditions and with augmented and diminished contractility, we found that a ~60% of the total energy of the backward expansion wave is spent in this deceleration.

Limitations. As discussed in our previous study (36), the application of one-dimensional WIA to LV filling is more problematic than it is in the large arteries. However, this concern should be minimal in the plane of the mitral valve. Mitral velocity was measured near the midpoint of the mitral annulus using Doppler echocardiography. This velocity should be representative of the entire cross section in that the velocity profile is blunt in early diastole (31, 34).

So that we could compare the fractions of aspirating energy utilized for stroke volume deceleration and DS, we calculated wave intensity from a single P_{LV} that was measured between the mitral and aortic valves. This violated the wave-intensity principle that pressure and velocity should be recorded from the same cross section. As there are measurable gradients in the LV during diastolic filling (13), our results might be somewhat different quantitatively from those derived from P_{LV}s measured precisely within the mitral orifice, for example. Further experiments are planned to define these differences.

This was an ambitious experimental protocol in which we studied several interventions and measured many parameters in these anesthetized dogs. Probably as a result, the ejection fraction was low and P_{Peric} was higher than we have usually observed and a degree of cardiac depression may have been present in these dogs. It will be important to confirm the most important results of this study in more physiological animal models and/or in human subjects.

With respect to clinical studies, we acknowledge that our measurements were profoundly "invasive" and we do not mean to suggest that our approach is easily adaptable to the clinical laboratory. The ultimate goal of our experimental investigations is to understand the mechanisms that produce the normal and abnormal patterns of mitral and pulmonary venous velocity. With that understanding, we believe that future cardiologists will be able to interpret the clinical patterns more intelligently.

In conclusion, the intensity of the backward-going wave generated by the LV during relaxation depends both on the rate at which E decreases (i.e., τ) and on the completeness of LV emptying (i.e., V_{LVES}). Wave-intensity analysis provides a new approach for assessing diastolic suction and reconciles those two previously proposed mechanisms. The early filling wave (E wave) depends on DS in addition to the passive decompression of the LA.

APPENDIX

To attempt to demonstrate that a backward-going expansion wave could be generated by decreasing E in the absence of elastic recoil (i.e., a V_0 mechanism), we connected two water-containing flaccid toy balloons via a Silastic rubber tube (Fig. 9, *top*). Pressures were measured in the balloons (P_A, P_B) and at a point in the tube where velocity was also measured (P, U). The balloons were contained
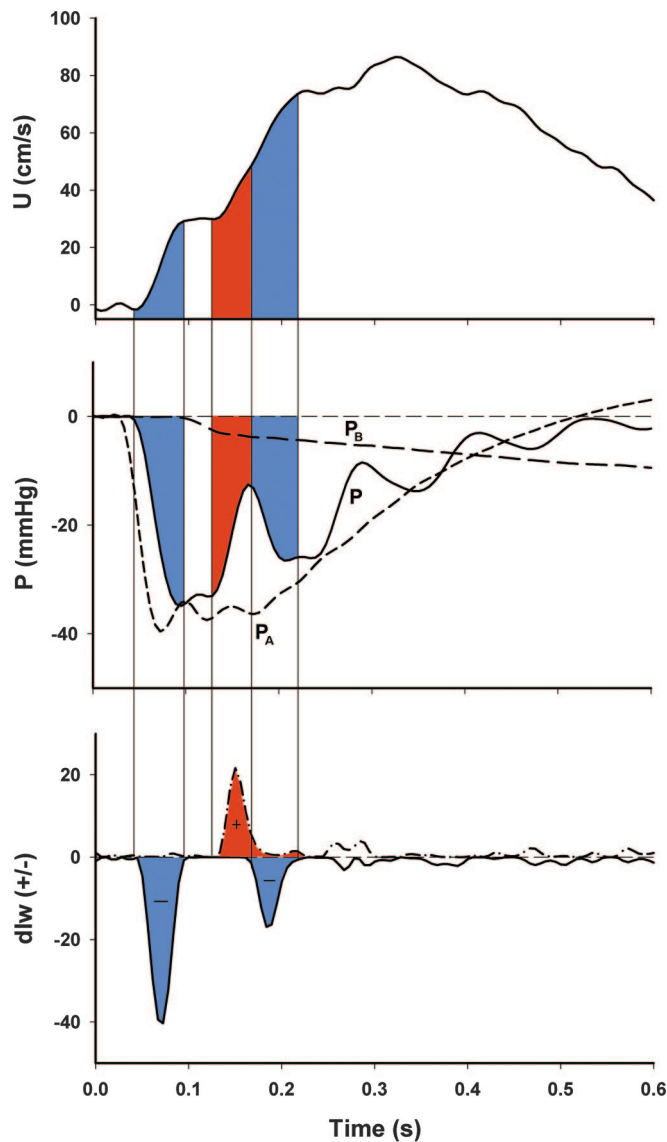

Fig. 9. A diagram of a bench-top experiment in which two water-containing, flaccid, toy balloons were connected via a rigid tube (*top*). Balloons were enclosed in interconnected air-filled bottles that were initially pressurized to end-systolic levels. Manipulation of clamps allowed P_A to fall suddenly to zero while P_B remained high. Wave intensity analysis (*bottom*) of pressure (P) and velocity (U) changes in the tube yielded an initial backward-going expansion wave (BEW; expansion waves are indicated in blue). After a brief pause during which no waves were present, U and P increased. These changes were caused by a forward compression wave (FCW; red), which was due to the negative (open-ended) reflection of the initial BEW. Then, as U continued to increase, P decreased. These changes were caused by a second BEW, which was also due to negative (open-ended) reflection, this time of the preceding FCW.

within interconnected air-filled bottles that were initially equally pressurized to end-systolic levels. Manipulation of clamps allowed P_A to fall suddenly to zero (thus simulating ventricular relaxation) while P_B remained high. This resulted in a backward-going expansion wave that accelerated the column of water toward the first balloon. In that there was no V_0 mechanism and the decompression of *bottle A* decreased that balloon's E ($\Delta P/\Delta V$), we suggest that decreasing elastance, per se, caused the backward-going expansion wave. WIA also defined negatively reflected compression and expansion waves (21).

REFERENCES

1. **Bell SP, Fabian J, Higashiyama A, Chen Z, Tischler MD, Watkins MW, and LeWinter MM.** Restoring forces assessed with left atrial pressure clamps. *Am J Physiol Heart Circ Physiol* 270: H1015–H1020, 1996.
2. **Bell SP, Fabian J, and LeWinter MM.** Effects of dobutamine on left ventricular restoring forces. *Am J Physiol Heart Circ Physiol* 275: H190–H194, 1998.
3. **Beyar R, Yin FCP, Hausknecht M, Weisfeldt ML, and Kass DA.** Dependence of left ventricular twist-radial shortening relations on cardiac cycle phase. *Am J Physiol Heart Circ Physiol* 257: H1119–H1126, 1989.
4. **Bloom WL.** Diastolic filling of the beating excised heart. *Am J Physiol* 187: 143–144, 1955.
5. **Bloom WL and Ferris EB.** Negative ventricular diastolic pressure in beating heart studied in vitro and in vivo. *Proc Soc Exp Biol Med* 93: 451–454, 1956.
6. **Bowman AW and Kovacs SJ.** Left atrial conduit volume is generated by deviation from the constant-volume state of the left heart: a combined MRI-echocardiographic study. *Am J Physiol Heart Circ Physiol* 286: H2416–H2424, 2004.
7. **Brecher GA.** Experimental evidence of ventricular diastolic suction. *Circ Res* 4: 513–518, 1956.
8. **Brecher GA.** Critical review of recent work on ventricular diastolic suction. *Circ Res* 6: 554–566, 1958.
9. **Brecher GA and Kissen AT.** Relation of negative intraventricular pressure to ventricular volume. *Circ Res* 5: 157–162, 1957.
10. **Brecher GA and Kissen AT.** Ventricular diastolic suction at normal arterial pressures. *Circ Res* 6: 100–106, 1958.
11. **Chen C, Rodriguez L, Levine RA, Weyman AE, and Thomas JD.** Noninvasive measurements of the time constant of left ventricular relaxation using the continuous wave doppler velocity profile of mitral regurgitation. *Circulation* 86: 272–278, 1992.
12. **Choong CY, Abascal VM, Thomas JD, Guerrero JL, McGlew S, and Weyman AE.** Combined influence of ventricular loading and relaxation on the transmitral flow velocity profile in dogs measured by Doppler echocardiography. *Circulation* 78: 672–683, 1988.
13. **Courtois M, Kovacs SJ Jr, and Ludbrook PA.** Transmitral pressure-flow velocity relation: importance of regional pressure gradients in the left ventricle during diastole. *Circulation* 78: 661–671, 1988.
14. **Dong SJ, Beyar R, Zhou ZN, Fick GH, Smith ER, and Tyberg JV.** Determinants of midwall circumferential segmental length of the canine ventricular septum at end diastole. *Am J Physiol Heart Circ Physiol* 265: H2057–H2065, 1993.
15. **Firstenberg MS, Smedira NG, Greenberg NL, Prior DL, McCarthy PM, Garcia MJ, and Thomas JD.** Relationship between early diastolic intraventricular pressure gradients, an index of elastic recoil, and improvements in systolic and diastolic function. *Circulation* 104: I330–I335, 2001.
16. **Fowler NO, Bloom WL, and Ferris EB.** Systolic-diastolic pressure relationships in the isolated beating heart. *Circ Res* 5: 485–488, 1957.
17. **Fowler NO, Shabetai R, and Braunstein JR.** Transmural ventricular pressures in experimental cardiac tamponade. *Circ Res* 7: 733–739, 1959.
18. **Hamilton DR, Dani RS, Semlacher RA, Smith ER, Kieser TM, and Tyberg JV.** Right atrial and right ventricular transmural pressures in dogs and humans. Effects of the pericardium. *Circulation* 90: 2492–2500, 1994.
19. **Hamilton DR, deVries G, and Tyberg JV.** Static and dynamic operating characteristics of a pericardial balloon. *J Appl Physiol* 90: 1481–1488, 2001.
20. **Hollander EH, Dobson GM, Wang JJ, Parker KH, and Tyberg JV.** Direct and series transmission of left atrial pressure perturbations to the pulmonary artery: a study using wave-intensity analysis. *Am J Physiol Heart Circ Physiol* 286: H267–H275, 2004.
21. **Hollander EH, Wang JJ, Dobson GM, Parker KH, and Tyberg JV.** Negative wave reflections in pulmonary arteries. *Am J Physiol Heart Circ Physiol* 281: H895–H902, 2001.
22. **Hori M, Yellin EL, and Sonnenblick EH.** Left ventricular diastolic suction as a mechanism of ventricular filling. *Jpn Circ J* 46: 124–129, 1982.
23. **Ingels NB Jr, Daughters GT, II, Nikolic SD, DeAnda A, Moon MR, Bolger AF, Komeda M, Derby GC, Yellin EL, and Miller DC.** Left atrial pressure-clamp servomechanism demonstrates LV suction in canine hearts with normal mitral valves. *Am J Physiol Heart Circ Physiol* 267: H354–H362, 1994.
24. **Ingels NB Jr, Daughters GT, Nikolic SD, DeAnda A, Moon MR, Bolger AF, Komeda M, Derby GC, Yellin EL, and Miller DC.** Left ventricular diastolic suction with zero left atrial pressure in open-chest dogs. *Am J Physiol Heart Circ Physiol* 270: H1217–H1224, 1996.
25. **Janssen PML and de Tombe PP.** Uncontrolled sarcomere shortening increases intracellular Ca^{2+} transient in rat cardiac trabeculae. *Am J Physiol Heart Circ Physiol* 272: H1892–H1897, 1997.
26. **Johnston WE, Vinten-Johansen J, Tommasi E, and Little WC.** ULFS-49 causes bradycardia without decreasing right ventricular systolic and diastolic performance. *J Cardiovasc Pharmacol* 18: 528–534, 1991.
27. **Jones CJH, Parker KH, Hughes R, and Sheridan DJ.** Nonlinearity of human arterial pulse wave transmission. *J Biomech Eng* 114: 10–14, 1992.
28. **Jones CJH, Sugawara M, Davies RH, Kondoh Y, Uchida K, and Parker KH.** Arterial wave intensity: physical meaning and physiological significance. In: *Recent Progress in Cardiovascular Mechanics*, edited by Hosoda S, Yaginuma T, Sugawara M, Taylor MG and Caro CG. Chur, Switzerland: Harwood, 1994, p. 129–148.
29. **Kass DA, Bronzwaer JG, and Paulus WJ.** What mechanisms underlie diastolic dysfunction in heart failure? *Circ Res* 94: 1533–1542, 2004.
30. **Katz LN.** The role played by the ventricular relaxation process in filling the ventricle. *Am J Physiol* 95: 542–553, 1930.
31. **Kim WY, Walker PG, Pedersen EM, Poulsen JK, Oyre S, Houlind K, and Yoganathan AP.** Left ventricular blood flow patterns in normal subjects: a quantitative analysis by three-dimensional magnetic resonance velocity mapping. *J Am Coll Cardiol* 26: 224–238, 1995.
32. **Kovacs SJ, McQueen DM, and Peskin CS.** Modelling cardiac fluid dynamics and diastolic function. *Philos Trans R Soc Lond A Math Phys Sci* 359: 1299–1314, 2001.
33. **Kroeker CAG, Tyberg JV, and Beyar R.** The effects of load manipulations, heart rate, and contractility on apical rotation: an experimental study in anaesthetized dogs. *Circulation* 92: 130–141, 1995.
34. **Kupari M, Jarvinen V, Poutanen VP, and Hekali P.** Skewness of instantaneous mitral transannular flow-velocity profiles in normal humans. *Am J Physiol Heart Circ Physiol* 268: H1232–H1238, 1995.
35. **Lighthill MJ.** *Waves in Fluids.* Cambridge: Cambridge University Press, 1978.
36. **MacRae JM, Sun YH, Isaac DL, Dobson GM, Cheng CP, Little WC, Parker KH, and Tyberg JV.** Wave-intensity analysis: a new approach to left ventricular filling dynamics. *Heart Vessels* 12: 53–59, 1997.
37. **Nikolic S, Yellin EL, Tamura K, Vetter H, Tamura T, Meisner JS, and Frater RWM.** Passive properties of canine left ventricle: diastolic stiffness and restoring forces. *Circ Res* 62: 1210–1222, 1988.
38. **Ohno M, Cheng CP, and Little WC.** Mechanism of altered patterns of left ventricular filling during the development of congestive heart failure. *Circulation* 89: 2241–2250, 1994.
39. **Parker KH and Jones CJH.** Forward and backward running waves in the arteries: analysis using the method of characteristics. *J Biomech Eng* 112: 322–326, 1990.
40. **Parker KH, Jones CJH, Dawson JR, and Gibson DG.** What stops the flow of blood from the heart? *Heart Vessels* 4: 241–245, 1988.
41. **Rademakers FE, Buchalter MB, Rogers WJ, Zerhouni EA, Weisfeldt ML, Weiss JL, and Shapiro EP.** Dissociation between left ventricular untwisting and filling. Accentuation by catecholamines. *Circulation* 85: 1572–1581, 1992.
42. **Smiseth OA, Frais MA, Kingma I, Smith ER, and Tyberg JV.** Assessment of pericardial constraint in dogs. *Circulation* 71: 158–164, 1985.

43. **Smiseth OA, Thompson CR, Lohavanichbutr K, Abel JG, Miyagishima RT, Lichtenstein SV, and Bowering J.** The pulmonary venous systolic flow pulse–its origin and relationship to left atrial pressure. *J Am Coll Cardiol* 34: 802–809, 1999.

44. **Suga H, Goto Y, Igarashi Y, Yamada O, Nozawa T, and Yasumura Y.** Ventricular suction under zero source pressure for fillling. *Am J Physiol Heart Circ Physiol* 251: H47–H55, 1986.

45. **Sun YH, Anderson TJ, Parker KH, and Tyberg JV.** Wave-intensity analysis: a new approach to coronary dynamics. *J Appl Physiol* 89: 1636–1644, 2000.

46. **Sun YH, Sjoberg BJ, Ask P, Loyd D, and Wranne B.** Mathematical model that characterizes transmitral and pulmonary venous flow velocity patterns. *Am J Physiol Heart Circ Physiol* 268: H476–H489, 1995.

47. **Thomas JD and Weyman AE.** Echocardiographic Doppler evaluation of left ventricular diastolic function. Physics and physiology. *Circulation* 84: 977–990, 1991.

48. **Tyberg JV, Keon WJ, Sonnenblick EH, and Urschel CW.** Mechanics of ventricular diastole. *Cardiovasc Res* 4: 423–428, 1970.

49. **Vierendeels JA, Riemslagh K, Dick E, and Verdonck PR.** Computer simulation of intraventricular flow and pressure gradients during diastole. *J Biomech Eng* 122: 667–674, 2000.

50. **Wang JJ, Parker KH, and Tyberg JV.** Left ventricular wave speed. *J Appl Physiol* 91: 2531–2536, 2001.

51. **Wiggers CJ.** Studies in the consecutive phases of the cardiac cycle. *Am J Physiol* 56: 415–459, 1921.

52. **Wiggers CJ.** Cardiac mechanisms that limit operation of ventricular suction. *Science* 126: 1237, 1957.

American Journal of Physiology – Heart and Circulatory Physiology

Corrigendum
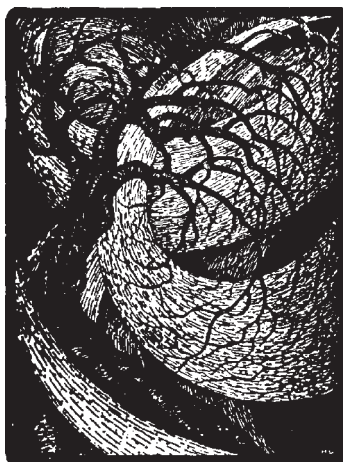
Volume 288, April 2005
Volume 57, April 2005

Pages H1641-H1651: Wang Z, F Jalali, Y-H Sun, J-J Wang, KH Parker, and JVTyberg. "Assessment of left ventricular diastolic suction in dogs using wave-intensity analysis." A diagram of a bench-top experiment in Figure 9 was missing. Figure 9 should appear as the following.

H3017